

The round thermal jet: undisturbed and in cross-flow

LEIF N. PERSEN and HENRY ØIANN

Institutt for Mekanikk, University of Trondheim, NTH, Trondheim, Norway

and

HIMADRI P. MAZUMDAR

Indian Statistical Institute, Calcutta, India

(Received 22 June 1990 and in final form 18 June 1992)

Abstract—This paper investigates the round jet exiting from a cut-off circular pipe into still air. It examines the similarity properties in the same way as the senior author has done for the two-dimensional jet. The same type of relations are found as in the previous case. It can be concluded that the free turbulence exhibits no relation with the jet's Reynolds number and that consequently the nozzle geometry exclusively governs the flow. The case of a heated circular jet is incorporated in the investigation and the same conclusions are drawn for the temperature field as for the velocity field. The result throws light on the dispute between Taylor and Prandtl regarding the mixing length in the two fields. The second part of the paper examines the similarity properties of the temperature field of the jet when it exits into a cross-flow of different temperature.

INTRODUCTION

THE THERMAL jet has been the subject of numerous investigations, of which only a very limited number will be drawn to attention here [1-5]. Perhaps the most fundamental study was undertaken by van der Hegge Zijnen [4], who in a series of investigations studied the convection of mass, momentum and energy in a jet flow using a plane jet. The investigation which perhaps is most closely related to the present one was done by Kamotani and Greber [6], who also give an extensive list of relevant papers.

The first part of the present investigation is concerned with the undisturbed thermal jet and the possibility of describing the thermal jet in the same way as was previously done by the senior author [7] in the treatment of the jet's velocity field. The essence of this treatment is the realization of the fact that the jet's flow field (in the absence of fixed walls) is independent of the Reynolds number (and thus also of viscosity) and in the near field is entirely determined by geometry. Secondly, the similarity features of the jet are studied. The same behavior will be shown to apply also to the near field of the thermal jet and the similarity features of the thermal jet will be scrutinized.

The second part of the investigation is concerned with the thermal jet in cross-flow. It will be shown that the similarity features of the thermal jet go beyond what has hitherto been described in ref. [6].

Because of the close connection to the investigation by Kamotani and Greber [6], a few comments ought to be made. These authors find what they describe

as 'a remarkable self-similarity' in the downstream temperature profile when measured in the central plane (shown in Fig. 1) for a jet in cross-flow. However, the maximum temperature measured in the central plane is not necessarily the maximum temperature in the cross-section in which these profiles are measured. Such maxima may, under certain conditions, lie in pairs on either side of the central plane, as indicated by the isotherms sketched in the cross-sectional plane in Fig. 1.

The velocity field of the wake behind the pipe from which the thermal jet is exiting has been thoroughly

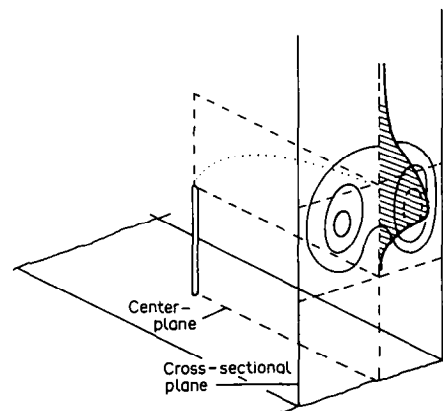


Fig. 1. Sketch of the temperature profile as measured in the central plane.

investigated by Schatzmann [3], and consequently the emphasis here is put on the temperature field of the thermal jet.

The spread of the jet and the decay of the centerline temperature were used by Kamotani and Greber [6] as quantities representative of the description of the thermal jet. This will also be done here, but attention is drawn to the fact that their method of non-dimensionalizing their results differs from that used in the present investigation. The latter method is believed to represent an improvement.

THE MEASUREMENTS (FREE JET) AND THEIR EVALUATION

The free jets under investigation were created by letting a stream of hot air exit from the end of a tube into still air. The exit geometry is the simplest possible: the tube is cut perpendicular to the tube's axis. Two different tube diameters are used: 44 mm and 27 mm. The elements used to heat the air had three different stages, making it possible to vary the exit temperature. The exit velocity could also be set at three different levels. This should provide a reasonable range of variation to give the investigation the necessary generality. The characteristics of the first 10 cases in the investigation are given in Table 1. The exit velocities are either 'normal', 'low' or 'high', the exit temperature setting is given by the labels 'no' (isothermal conditions), 'T1', 'T2', 'W1' or 'W2'. These cases are subsequently verified by additional experiments, to be treated later.

For each of the cases in Table 1, eight to ten profiles were traversed perpendicular to the jet's axis at different distances from the exit. Each profile consisted of 20-40 points where velocity and temperature were recorded, giving a total of 1760-2640 data points. The evaluation of the results is based on the same procedure as used by the senior author [1] for the plane jet.

A typical profile for either temperature or velocity may look like the one sketched in Fig. 2, where the measured values are plotted as a function of the traversing coordinate (x). It is observed that the temperature is recorded as a difference (ΔT) between the

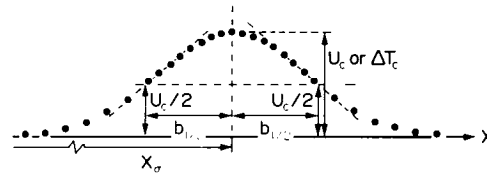


FIG. 2. Velocity or temperature profile (experimental).

measured value and the ambient temperature, whereas the velocity is simply the measured value since the jet exits into still air.

A parabola is fitted by a best fit procedure (least square) through the data points closest to the maximum. In this way the maximum value (the centerline value) itself and its location in the profile are easily found. The next step is to determine the half width ($b_{1,2}$ for the velocity and $B_{1,2}$ for the temperature) by finding the coordinate at which a straight line through the data points around half the maximum value exhibits that value. This means that the procedure used will produce three parameters of the profile:

1. The location of the centerline: x_0, x_0 .
2. The centerline value of the profile: $U_c, \Delta T_c$.
3. The half width of the profile: $b_{1,2}, B_{1,2}$.

The half width of the profile is used to non-dimensionalize the traversing coordinate such that the location of the point at which the profile exhibits half the maximum value will always be $\eta = 1$, η being the non-dimensional traversing coordinate. The maximum value at the centerline (velocity or temperature) is used to normalize the data points and the profiles for a single case will then appear as shown in Fig. 3, where eight profiles are plotted on top of each other, thus exhibiting the well known self-similarity characteristics for the velocity field.

This means that *the main information about the velocity field is hidden in the dependence on the downstream coordinate of the three quantities:*

$$U_c, b_{1,2}, x_0.$$

Since the temperature profiles can be shown to yield to the same treatment, *the temperature field is determined in the same way by the dependence on the downstream coordinate of the quantities:*

Table 1

Case no.	Exit diam. (mm)	Exit velocity	Exit temperature
I	44	normal	no
II	44	normal	no
III	27	low	no
IV	27	high	no
V	44	normal	T1
VI	44	normal	T2
(VII)	—	—	—
VIII	44	normal	no
IX	27	low	W1
X	27	high	W1
XI	27	high	W2

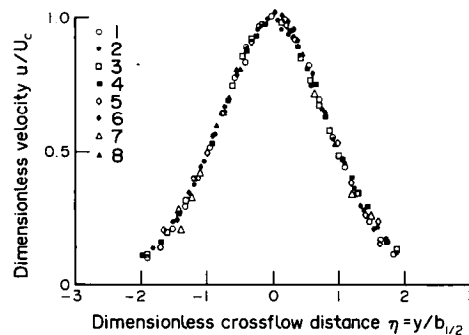


FIG. 3. Normalized velocity profiles.

$$\Delta T_c, B_{1/2}, x_0.$$

The downstream dependence of the quantities in question is now easily found by introduction of the evaluation procedure used in ref. [7]. The near field was shown to start a distance z_0 downstream of the exit, and to be adequately described by the following expressions (the velocity field):

$$\begin{aligned} U_c &= U_c^{(0)}[1 + \xi^2]^{-1/2} \\ b_{1/2} &= b_{1/2}^{(0)}[1 + \xi^2]^{1/2} \\ \xi &= (z - z_0)/L_{char}. \end{aligned} \quad (1)$$

Here three new parameters appear:

$U_c^{(0)}$ = the centerline velocity at the distance z_0 , downstream of which the jet becomes self-similar.

$b_{1/2}^{(0)}$ = the jet's half width at the distance z_0 .

L_{char} = the characteristic length of the jet with which the downstream distance is made dimensionless, thus normalizing the velocity field for all jets.

The same evaluation procedure as shown above for the velocity field is now applied to the temperature field. This means that from the temperature data the values of $B_{1/2}$ and ΔT_c are determined as explained in connection with Fig. 2. The temperature field is then given by:

$$\begin{aligned} \Delta T_c &= \Delta T_c^{(0)}[1 + \xi^2]^{-1/2} \\ B_{1/2} &= B_{1/2}^{(0)}[1 + \xi^2]^{1/2} \\ \xi &= (z - z_0^{(T)})/L_{char}^{(T)}, \end{aligned} \quad (2)$$

where the new parameters $T_c^{(0)}$, $B_{1/2}^{(0)}$ and $L_{char}^{(T)}$ are found from the temperature data by a best fit procedure.

The procedure is perhaps best understood from the examples given in Figs. 4-6. In Fig. 4 the values of U_c and $b_{1/2}$ for each profile in case I are plotted as functions of the downstream distance z . The curves representing these data are found by a best fit procedure.

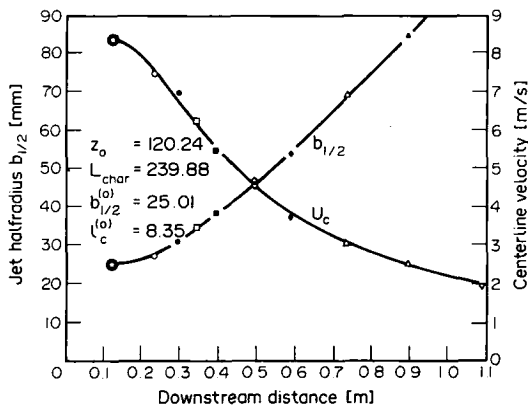


FIG. 4. The centerline velocity (U_c) and the jet's half width ($b_{1/2}$) as functions of the downstream distance (case I).

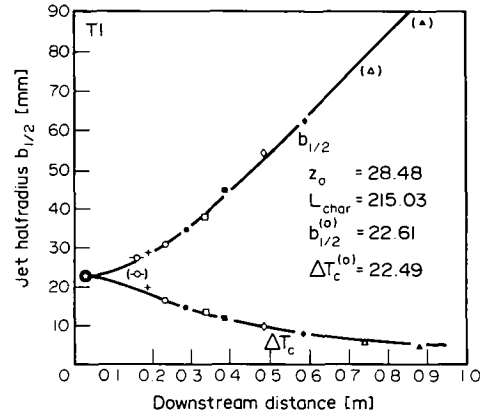


FIG. 5. The centerline temperature ΔT_c and the half width $B_{1/2}$ as functions of the downstream distance (case V).

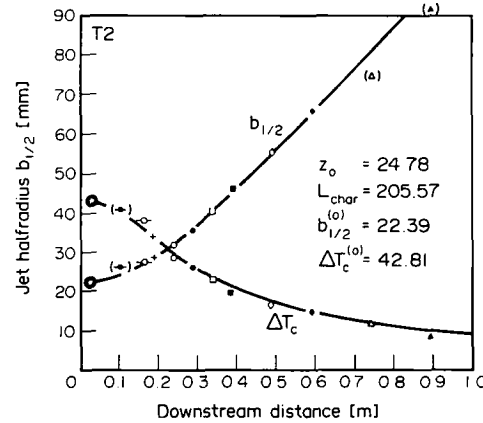


FIG. 6. The centerline temperature ΔT_c and the jet's half width $B_{1/2}$ as functions of the downstream distance (case VI).

thus determining the parameters of equations (1). The actual values are given in the diagram (distances in mm). It is remarkable how well the chosen curves represent the data.

In Figs. 5 and 6 the same procedure has been applied to the temperature data of cases V and VI respectively. Again, a seemingly good approximation to the experimental values is obtained through a proper choice of the parameters of equation (2).

The generality of this representation of the experimental findings can now only be made plausible by using the procedure to a variety of cases. Only if this is successful can this way of representing the flow field as well as the temperature field of a thermal jet be considered adequate.

QUESTIONS AND CONCLUSIONS

In connection with the investigation of the thermal jet a series of questions were asked and some answered. Here is a list of those questions.

- Q1. Does the half width really increase linearly with the downstream distance?

- A1. The half widths of the velocity and temperature fields seem to be very well represented by the hyperbolic function used to evaluate the data. Therefore, asymptotically, the linear increase of the half widths seems to be adequately supported, at least in the near field. Some indication has been observed that this conclusion may not be extended indefinitely downstream. In the far field additional information is therefore needed.
- Q2. Do the centerline values of the fields really decay with downstream distance by the power $-\frac{1}{2}$ as indicated in equations (1) and (2)?
- A2. All indications are that this is correct for the velocity field (for U_c) of the cold jet. However, it may be that the way in which the centerline values (U_c and ΔT_c) decay may depend on the exit temperature. The value of the exponent in the decay functions has therefore been set to $-n$ and the best fit value for n has been determined. The result of this procedure is shown in the table displaying the results. The following expressions are therefore substituted:

$$\begin{aligned} U_c &= U_c^{(0)}[1 + \xi^2]^{-n} \\ \Delta T_c &= \Delta T_c^{(0)}[1 + \xi^2]^{-n}. \end{aligned} \quad (3)$$

- Q3. Does buoyancy influence the results?
- A3. To avoid unwanted effects of an eventual influence, the free jet was directed vertically upwards. As far as the velocity fields were concerned, no influence could be traced in the data other than the one expressed through the exponent n , leaving the velocity field uninfluenced by temperature within the limits set by the temperature variations used in the investigation.

This last statement is perhaps best illustrated by the results exhibited in Fig. 7, where the results for the half width with a cold jet (cases I and II) and those with a hot jet (cases V, VI and VIII, different exit temperatures) are plotted together. The difference between the different cases is of the same order of

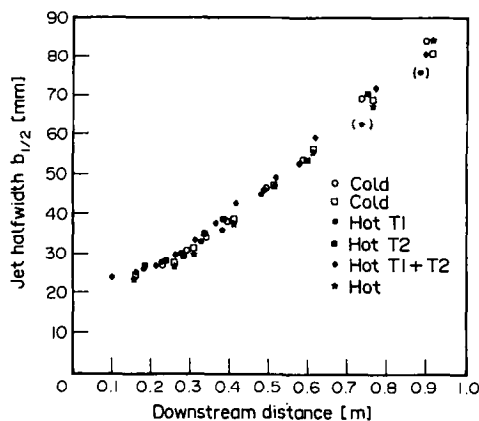


FIG. 7. All data for $b_{1/2}$ from cases I and II (cold jet) and from cases V, VI and VIII (hot jet) plotted as functions of downstream distance. Exit diameter 44 mm.

Table 2

Case	$U_c^{(0)}$	n	$(\Delta T_c^{(0)})$
V	8.586	0.5333	(24.70)
VI	9.066	0.5964	(41.83)
VIII	9.028	0.5492	(32.52)

magnitude as the accuracy of the measurements, thus lending strong support for the observation in statement A3.

Question Q2 may be illuminated by the results for cases V, VI and VIII. Table 2 shows the results of the evaluation procedure for these cases. It seems to indicate a dependence of n on the exit temperature (here indicated by $\Delta T_c^{(0)}$). This result will be further scrutinized later.

With these preliminary remarks the final results of the investigation will be exhibited.

FINAL RESULTS (FREE JET)

The results of the investigation as far as the free thermal jet is concerned are summed up as follows.

The velocity field

1. The velocity field of a free thermal jet exhibits the same self-similarity features as the isothermal (cold) jet.
2. The spreading of the jet seems not to be influenced by temperature (Fig. 7), at least within the limits of temperature variation in the present investigation (approx. 60°C).
3. The empirical description of the velocity field (derived from the present data and believed to be generally applicable) depends only on geometry, i.e. on the exit radius of the nozzle (tube).
4. From (3), it follows that the analytic description of the flow field is uniquely determined by equations (2):

$$\begin{aligned} U_c &= U_c^{(0)}[1 + \xi^2]^{-n} \\ b_{1/2} &= b_{1/2}^{(0)}[1 + \xi^2]^{1/2} \\ \xi &= (z - z_0)/L_{\text{char}}^{(v)}, \end{aligned} \quad (4)$$

where

$$\begin{aligned} z_0 &= 2.728 D_{\text{exit}} \\ L_{\text{char}}^{(v)} &= 5.596 D_{\text{exit}} \\ b_{1/2}^{(0)} &= L_{\text{char}}^{(v)}/10. \end{aligned} \quad (5)$$

The characteristic length of the velocity field ($L_{\text{char}}^{(v)}$) is different from the one which applies to the temperature field. The distance (z_0) to the point downstream of which similarity sets in is also different for the two fields, as will be emphasized subsequently. The velocity field is seen to be entirely determined through equations (4) and (5) as soon as the exit diameter is known, the only other quantity needed being the exit velocity ($U_c^{(0)}$).

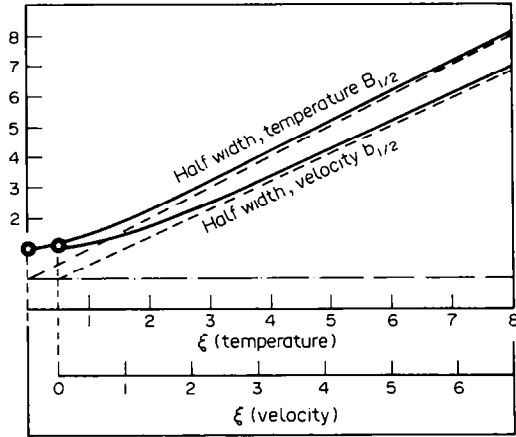


FIG. 8. Comparison between the spreading of the velocity and temperature fields of a circular jet using $b_{1/2}$ and $B_{1/2}$ as a measure.

The temperature field

1. The temperature field of a thermal jet exhibits the same self-similar features as the velocity field.
2. The temperature field is completely determined by :

$$\begin{aligned} \Delta T_c &= \Delta T_c^{(0)} [1 + \xi^2]^{-n^{(T)}} \\ B_{1/2} &= B_{1/2}^{(0)} [1 + \xi^2]^{1/2} \\ \xi &= (z - z_0^{(T)}) / L_{char}^{(T)}, \end{aligned} \quad (6)$$

where the parameters of the temperature field are :

$$\begin{aligned} z_0^{(T)} &= z_0^{(v)} - 0.35 L_{char}^{(T)} \\ L_{char}^{(T)} &= L_{char}^{(v)} / 1.11 \\ B_{1/2}^{(0)} &= L_{char}^{(T)} / 10. \end{aligned} \quad (7)$$

First, the difference in the spreading of the velocity and temperature fields is drawn to attention. Equation (7) shows how the two parameters L_{char} and z_0 not only differ but also depend on each other. This represents a conclusion drawn from the actual data of the investigation and Fig. 8 shows the effect of this difference. It is interesting to notice how this well known difference in the diffusion of momentum and energy comes about in the present presentation of the results.

Next, the exponent n of the decay functions is considered. Reference is made here to Table 3, where the results of the data evaluation are given in detail.

Figure 9 shows how n varies for both the velocity field and the temperature field. Reference is given to the two different pipe sizes from which the data originate. However, one should observe that the departure from the value $-\frac{1}{2}$ is small, at least for the temperature differences used in the present investigation. One might state that for practical purposes a conservative estimate of the centerline decay is found by using the value $-\frac{1}{2}$.

DETAILS OF THE DATA EVALUATION

The actual evaluation of the data is illustrated in Table 3, where the following procedure is implemented. First a hyperbola is fitted to all data for $b_{1/2}$ (or $B_{1/2}$) for the same exit diameter (D_{exit}). This leaves values for L_{char} and z_0 for both the velocity field and the temperature field. (The hyperbolas are defined in (4) and (6).) Next the values of these parameters are used when determining the curves (through a best fit procedure) which best represent the decay functions of the centerline quantities, i.e. the best fit values of the exponent n in these functions (equations (4) and

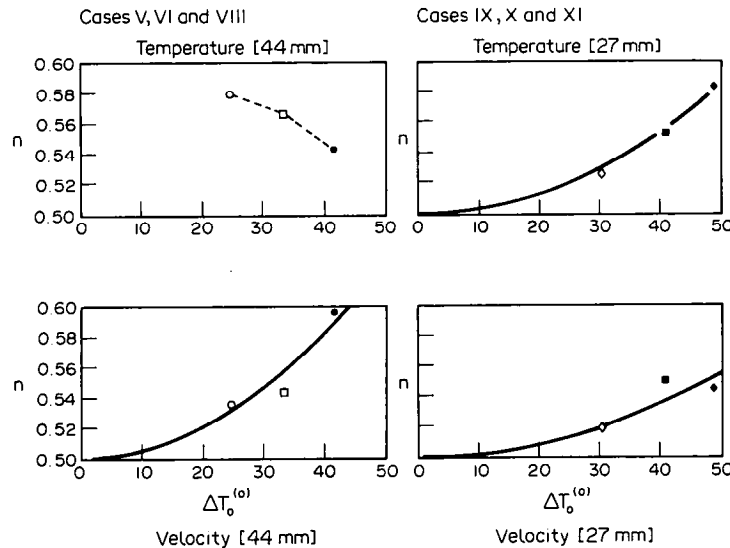


FIG. 9. Display of the dependence of the exponent n of the decay functions for the centerline velocity (U_c) and the centerline temperature (ΔT_c) on the exit temperature ($\Delta T_c^{(0)}$).

Table 3

Case no.	$z_0^{(r)}$	$L_{char}^{(r)}$	$b_{1/2}^{(0)}$	$U_c^{(0)}$	$n^{(r)}$	$z_0^{(T)}$	$L_{char}^{(T)}$	$B_{1/2}^{(0)}$	$\Delta T_c^{(0)}$	$n^{(T)}$	Remarks
I+II	117.75	236.00	24.41								Cold jet, $D_{exit} = 44$ mm
I				8.38	0.500						
II				8.91	0.500						
V+VI+VIII	119.27	238.72	24.41			39.99	212.54	23.09			Hot jet, $D_{exit} = 44$ mm
V				8.46	0.535				24.64	0.579	
VI				8.90	0.596				41.74	0.542	
VIII				8.84	0.543				33.20	0.566	
III+IV	94.24	167.78	16.26								Cold jet, $D_{exit} = 27$ mm
III				13.86	0.500						
IV				17.13	0.500						
IX+X+XI	68.05	163.34	15.91			83.82	148.69	18.21		0.553	Hot jet, $D_{exit} = 27$ mm
IX				16.07	0.551				40.98	0.553	
X				18.15	0.519				30.43	0.526	
XI				18.74	0.545				48.99	0.585	

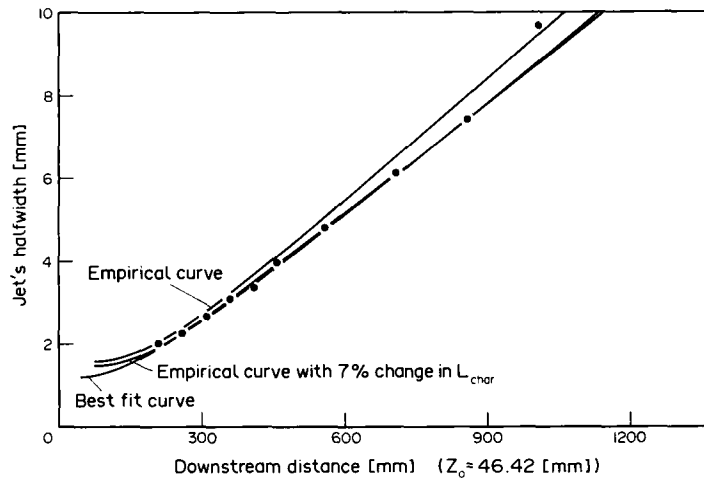


FIG. 10. The velocity field's half width as a function of downstream distance.

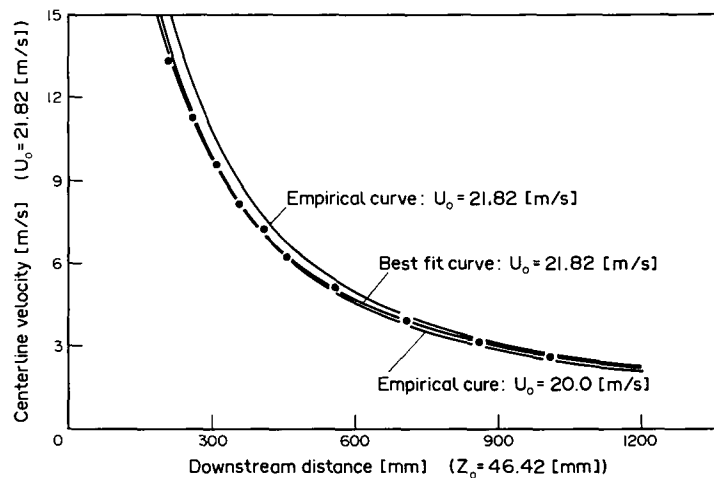


FIG. 11. The centerline velocity as a function of downstream distance.

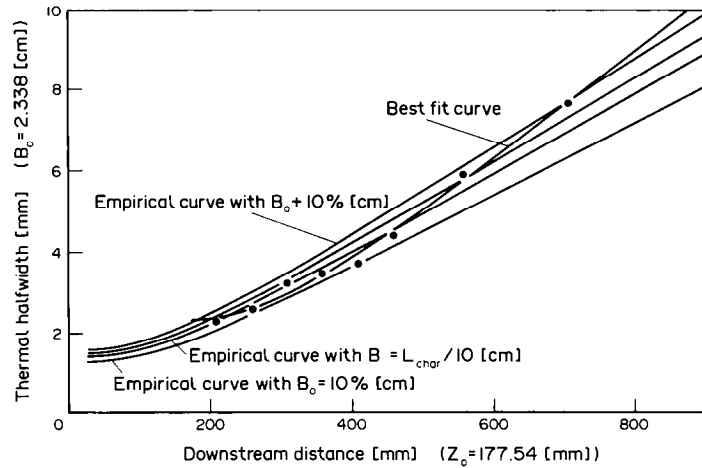


FIG. 12. The thermal half width as a function of downstream distance.

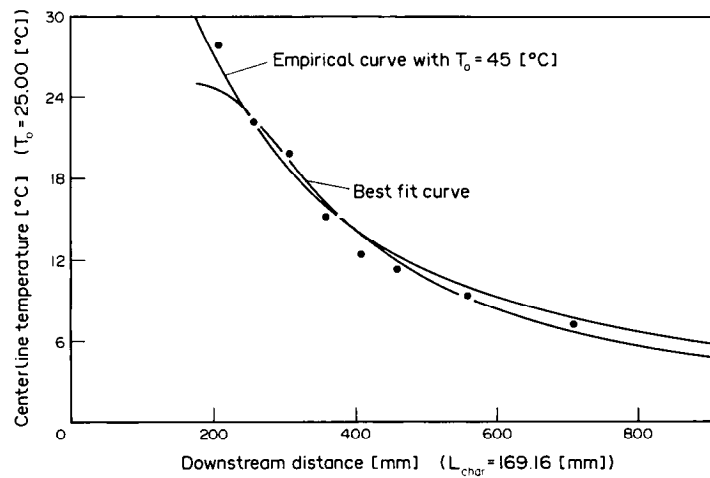


FIG. 13. The centerline temperature as a function of downstream distance.

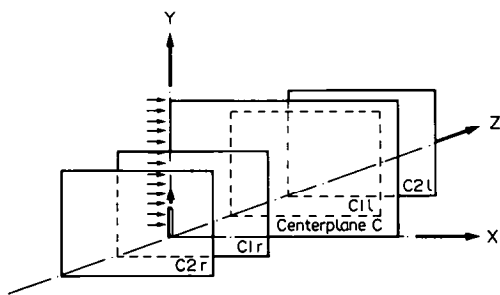


FIG. 14. Arrangement of the planes in which the profiles were measured.

(6) are determined. The results are shown in Table 3.

THE THERMAL JET IN CROSS-FLOW

Introduction

The experiments in cross-flow to be reported here were originally aimed exclusively at the question of to

what extent the similarity properties of the undisturbed jet could be traced in the fully three-dimensional flow of a jet in a cross-flow. The actual flow field has been investigated by Kamotani and Greber [6] and the emphasis was placed on the temperature field. To gain confidence in the accuracy of the experimental equipment, the undisturbed jet referred to earlier was considered. The complex flow field of the jet in cross-flow was then created in the wind tunnel of the Institutt for Mekanikk at the University of Trondheim.

The undisturbed jet

The experiment was conducted with a cut-off tube as the exit condition for the jet. The velocity field and the temperature field were investigated simultaneously using different probes for the two quantities. The evaluation procedure shown earlier was adopted, and gave the following results :

for the velocity field

$$b_{1/2} = 1.22 \text{ cm } (1.59 \text{ cm})$$

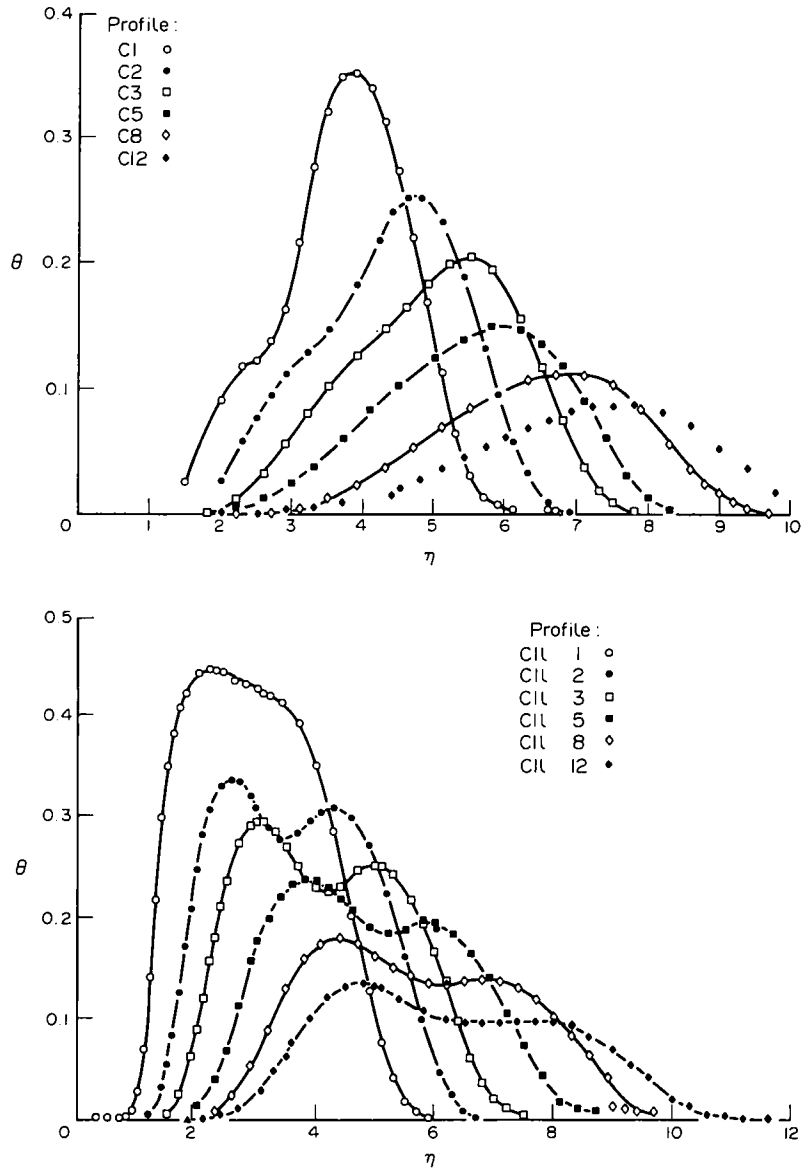


FIG. 15. Temperature profiles in the planes C and C1,l.

$$L_{char}^{(e)} = 135.35 \text{ mm} \quad (158.65 \text{ mm})$$

$$z_0^{(e)} = 46.42 \text{ mm} \quad (77.34 \text{ mm})$$

$$U_0 = 21.82 \text{ m s}^{-1}$$

$$n^{(e)} = 0.5332$$

for the temperature field

$$B_{1/2} = 2.34 \text{ cm} \quad (1.43 \text{ cm})$$

$$L_{char}^{(T)} = 169.16 \text{ mm} \quad (142.93 \text{ mm})$$

$$z_0^{(T)} = 177.54 \text{ mm} \quad (27.32 \text{ mm})$$

$$T_{co} = 25.00^\circ\text{C}$$

$$n^{(T)} = 0.5553.$$

The values in parentheses are those which can be computed from the generally valid empirical relations,

i.e. equations (4)–(7). The difference between the computed values and those evaluated from the experiment may seem large, but Figs. 10–13 reveal that the results are within a range of accuracy of 10%.

Figure 10 shows the data for the jet's half width (●) compared with the best-fit curve evaluated on the basis of the procedure given earlier. It is compared to the curve that is obtained from the empirical relations (5) with the exit diameter given as

$$D = 28.35 \text{ mm}.$$

Figure 11 shows how the data (●), the best-fit curve and the curve based on the empirical relations compare. It should be observed that as far as the empirical curves are concerned, the comparison is based on the jet's half width at the entrance being lowered by 7% and the jet's initial velocity by 9%. The results are judged to be satisfactory.

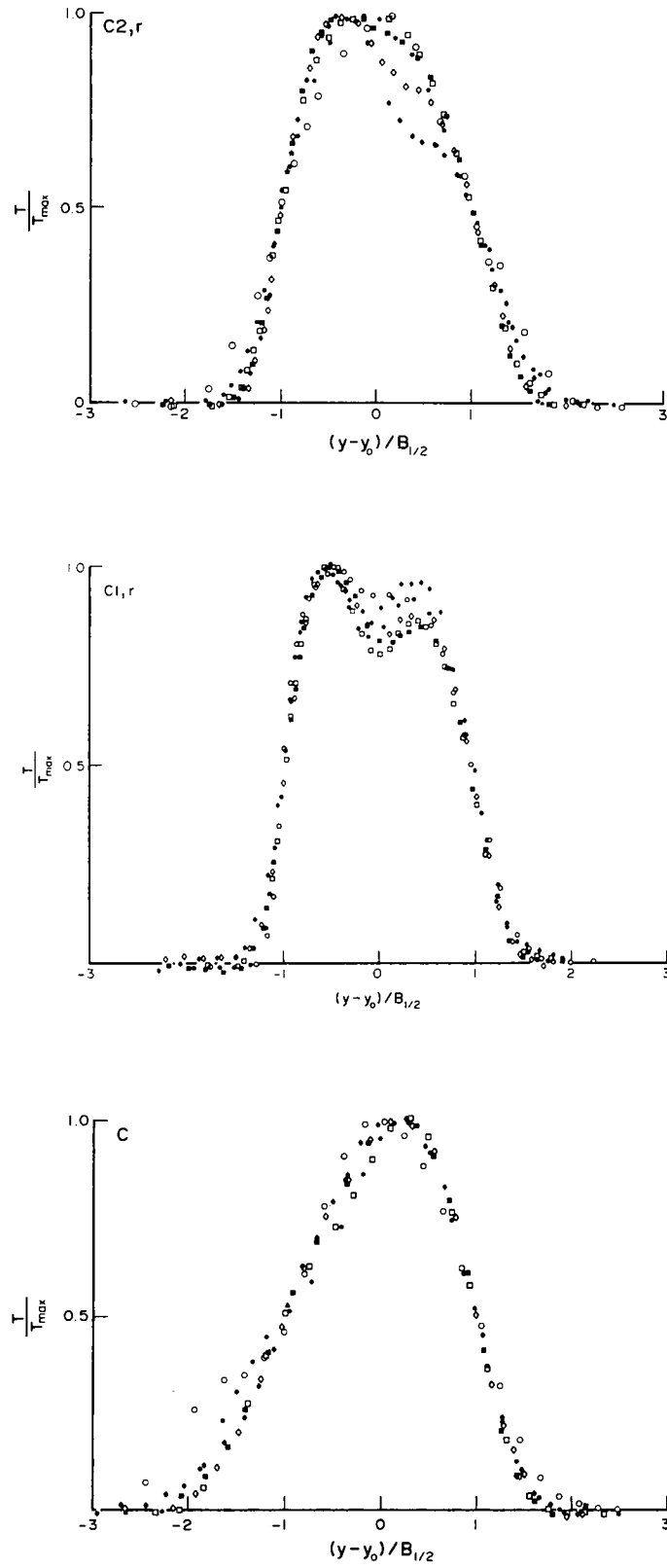


FIG. 16. Normalized temperature profiles in the four planes C2,r, C1,r, C and C1,l.

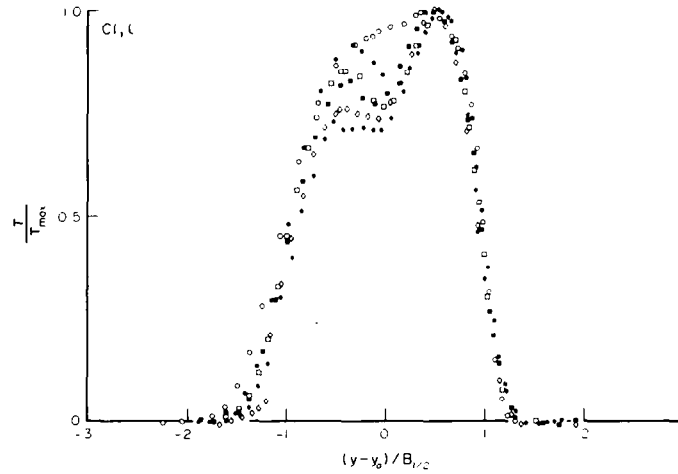


FIG. 16.—Continued.

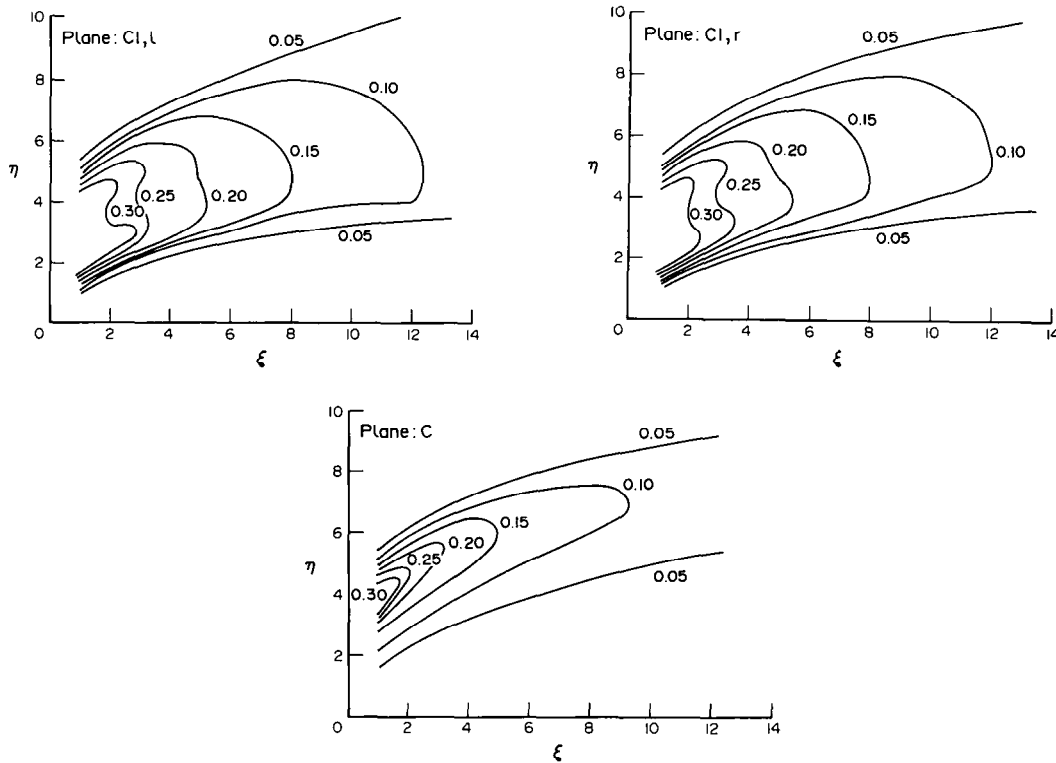


FIG. 17. Isotherms in the planes C1,r, C and C1,l.

Figures 12 and 13 show a comparison between the data (●), the best-fit curve and the curves based on the empirical relations for the temperature field. For the thermal half width the empirical value at the entrance has been reduced by 10% to obtain the agreement shown. For the entrance temperature, for which the empirical relations do not give an estimate (since it will depend on the exit temperature in each case),

the entrance temperature was 45°C. For the entrance velocity, the evaluated value of 21.82 m s⁻¹ was put at 20.0 m s⁻¹. It is acknowledged that the agreement is satisfactory.

The jet in cross-flow

As mentioned in the introductory remarks, the experimental set-up was obtained by letting a tube of

10 mm diameter extend approximately 20 cm from the floor of the wind tunnel into the flow in the wind tunnel of the Institutt for Mekanikk at Trondheim. Air from the shop was led into the cross-flow through the tube after having been heated in a water bed of constant temperature. The temperature was monitored to ensure that the temperature of the jet was constant and approximately 35 C above that of the flowing air in the tunnel. The temperature of the tunnel was kept constant by means of a heat exchanger in the tunnel, which extracted the heat created by the fan as well as that introduced through the jet escaping from the tube. It was verified that the experimental set-up gave a steady state situation of a thermal jet in cross-flow.

Temperature profiles perpendicular to the main stream of the wind tunnel at different distances from the tube were measured in the center plane (defined by the axes of the tube and the wind tunnel) as well as in two planes adjacent to it on each side, as shown in Fig. 14. The distance between the planes was 10 mm.

The exit conditions for the jet were kept constant from day to day. The variations were so small that they may be considered insignificant :

$$\begin{aligned} \text{Exit velocity} &: 34.8 \text{ m s}^{-1} \pm 0.5\% \\ \text{Exit temperature} &: 55.7 \text{ C} \pm 0.5\%. \end{aligned}$$

These quantities were measured immediately before and after each profile. The wind tunnel speed was set at 8.1 m s^{-1} .

The x -position of the profiles was the same in all planes and varied such that

$$\xi = x/d = 1, 2, 3, 5, 8 \text{ and } 12, \quad (8)$$

where d is the pipe diameter. The six profiles in each plane were sufficient to define the temperature field.

The data obtained consisted of the temperature T and the y -position at which it is measured. These data are made dimensionless as follows :

$$\theta = \frac{T - T_x}{T_c - T_x}, \quad \eta = y/d. \quad (9)$$

When θ is plotted vs η , one obtains the dimensionless temperature profiles shown in Fig. 15, where all profiles of planes C and C1,1 are plotted on top of each other.

It is obvious from the profiles that the pipe from which the jet exists is giving off some heat, thus cre-

ating the asymmetry of the profiles. This is most pronounced in the center plane and hardly noticeable in the C1,1 plane. In the latter one observes a second maximum value for the temperature, a fact that must be attributed to the influence of the vortices in the flow field [6].

The similarity properties of the temperature field are best examined if the evaluation procedure used for the data of the straight jet (described in detail earlier) is also applied to the present profiles. This means that the data from each profile will give the maximum value of the temperature T_{\max} , the position of the profiles center y_0 (defined through the half widths) and the half width itself $B_{1,2}$. The profiles are then normalized by plotting T/T_{\max} vs the non-dimensional transverse distance $(y - y_0)/B_{1,2}$.

The result is shown in Fig. 16 for four of the planes. The profiles show a remarkable self-similarity in view of the rather complex velocity field in which they are obtained. It is recalled that the flow field exhibits vortices which create irregularities in the temperature profiles on each side of the center plane, as Fig. 16 clearly shows. The fact that hotter regions may be found on each side of the center plane has already been shown by the diagrams in Fig. 15.

Finally, the resulting temperature field is examined by plotting the isotherms in the three middle planes as shown in Fig. 17. These isotherms ($\theta = \text{constant}$) emphasize the fact that the heat from the nozzle is convected more in the regions on both sides of the center plane than in the center plane itself.

REFERENCES

1. H. Reichardt, Zur Problematik der turbulent Strahl-ausbreitung in einer Grundströmung, *Mitteilungen Max-Planck Inst. Str. Forsch.* No. 35 (1965).
2. L. Fink, Strahl in turbulenzarmer und turbulenter Grundströmung, Dissertation, Universität Karlsruhe (1975).
3. M. Schatzmann, Auftriebstrahlen in natürlichen strömungen Entwicklung eines mathematischen Modells, Dissertation, Universität Karlsruhe (1976).
4. B. G. van der Hegge Zijnen, Measurements of the velocity distribution on a plane turbulent jet of air, *Appl. Sci. Res. Sec. A* 7, 256-275 (1947/49).
5. G. Webel, Berichtsliste des Sonderforschungsbereichs 80, Dissertation, Universität Karlsruhe (1981).
6. Y. Kamotani and I. Greber, Experiments on a turbulent jet in cross flow, *AIAA J.* 10, 1425-1429 (1972).
7. L. N. Persen, The near field of a plane turbulent jet, AGARD CP No. 308 (1981).